Advances in infrasonic remote sensing methods

J. D. Assink, P. S. M. Smets, O. Marcillo, C. Weemstra, J.-M. Lalande, R. Waxler,
L. G. Evers

Abstract Infrasound recordings can be used as input to inversion procedures to delineate the vertical structure of temperature and wind in a range of altitudes where ground based or satellite measurements are rare and where fine-scale atmospheric structures are not resolved by the current atmospheric specifications. As infrasound is measured worldwide, this allows for a remote sensing technique that can be applied globally. This chapter provides an overview of recently developed infrasonic remote sensing methods. The methods range from linearized inversions to direct search methods as well as interferometric techniques for atmospheric infrasound. The evaluation of numerical weather prediction (NWP) products shows the added value of infrasound, e.g. during Sudden Stratospheric Warming (SSW) and equinox periods. The potential transition towards assimilation of infrasound in numerical weather prediction models is discussed.

Jelle Assink, Pieter Smets and Läslo Evers
R&D Seismology and Acoustics, Royal Netherlands Meteorological Institute (KNMI),
P.O. Box 201, 3730 AE De Bilt, The Netherlands e-mail: assink@knmi.nl

Pieter Smets, Kees Weemstra and Läslo Evers
Dept. of Geoscience and Engineering, Faculty of Civil Engineering and Geosciences, Delft University of Technology, Stevinweg 1, 2628 CN Delft, The Netherlands

Omar Marcillo
EES-17, Geophysics Group,
Los Alamos National Laboratory Los Alamos, NM 87545, United States

Jean-Marie Lalande and Roger Waxler
National Center for Physical Acoustics,
University of Mississippi University, MS, 38677, United States

1 Introduction

Atmospheric specifications in the lower and middle atmosphere are routinely used in a wide variety of atmospheric sciences and its applications and are produced by NWP models. To initialise and constrain such models, data throughout the atmosphere is assimilated.

Various techniques exist that allow for in-situ measurements of atmospheric properties. Radiosondes provide accurate wind and temperature profiles up to the lower stratosphere (near 30 km), but the information is limited to one location and the uncertainty in the measurements increases in the lower stratosphere. On a nearly global scale, satellite-based instruments allow for the indirect estimation of temperature and horizontal winds up to an altitude of about 50 km (e.g., AMSU-A). As no direct measurements are available in the region above 30 km, winds are determined through the use of the thermal wind relation, which couples the vertical gradient in wind to the horizontal gradient in temperature. This leads to numerical problems in the tropics, as the Coriolis parameter vanishes at these latitudes. Moreover, biases in satellite measurements - especially in the higher stratosphere - are of particular concern, as this may have an adverse effect on weather forecasts, even for near-term forecasts. This is further discussed in the chapter by Lee et al. (this volume).

While the influence of the troposphere on the stratosphere is well-known, observational and modeling studies (Shaw and Shepherd, 2008) have demonstrated that the stratosphere has an impact on the troposphere as well. Weather and climate forecasters are moving towards a more comprehensive representation of the atmosphere, in order to capture the stratospheric-tropospheric interactions, which could enhance long-term forecasts. Therefore, there is a current interest in the NWP community to validate model specifications at stratospheric altitudes using independent observations (Randel et al, 2004). This includes the analysis of potential satellite radiance measurement biases, the consideration of additional high-resolution measurements (gravity waves, momentum flux) that are currently not resolved in the model runs, and validation of currently employed gravity wave model parameterization schemes (Charlton-Perez et al, 2013).

One of the techniques that is useful for such evaluations is low-frequency acoustic sounding. As infrasound waves propagate over long distances through the troposphere, stratosphere and mesosphere, infrasound recordings contain valuable information about the state of the atmosphere aloft (Figure 1). The earliest uses of this technique date back to a century ago (Fujiwhara, 1916; Whipple, 1926). Today, various remote sensing techniques have surpassed acoustics in the determination of atmospheric properties at the spatio-temporal scales that are of interest for NWP.

However, the impact of the middle atmosphere on enhanced long-term weather forecasts and the relative inaccessibility of this region has lead to a renewed interest in alternative remote sensing techniques. Recently, significant advances have been made in the development of acoustic remote sensing techniques to probe inaccessible regions of the atmosphere with a very high spatio-temporal resolution. The presence of a worldwide infrasound network, including facilities from the Interna-

tional Monitoring System (IMS), has been useful as it provides an opportunity to monitor atmospheric wind and temperature on a regional to global scale.

Infrasonic remote sensing is not only useful for improving weather models, but can be beneficial for applications that require a precise modeling, such as for estimation of explosion location and magnitude. Atmospheric specifications are based on spatio-temporally averaged measurements that often do not fully explain infrasound observations. The first step comprises of the estimation of atmospheric updates to explain traveltime, trace velocity and azimuth. Hereafter, signal duration can be used as independent variable to estimate source yield (Kulichkov, 2002; Lonzaga et al, 2015).

The remainder of this chapter is organized as follows. Section 2 provides a brief background of the sensitivity of infrasound to the atmosphere and discusses the relation between infrasound observables and temperature and wind. An overview of inverse methods for the estimation of temperature and wind profiles from infrasound data is discussed in Section 3. The potential of the infrasonic remote sensing method for NWP models is discussed in Section 4. Research in the field of interferometric techniques is discussed in Section 5. Finally, Section 6 summarizes the chapter.
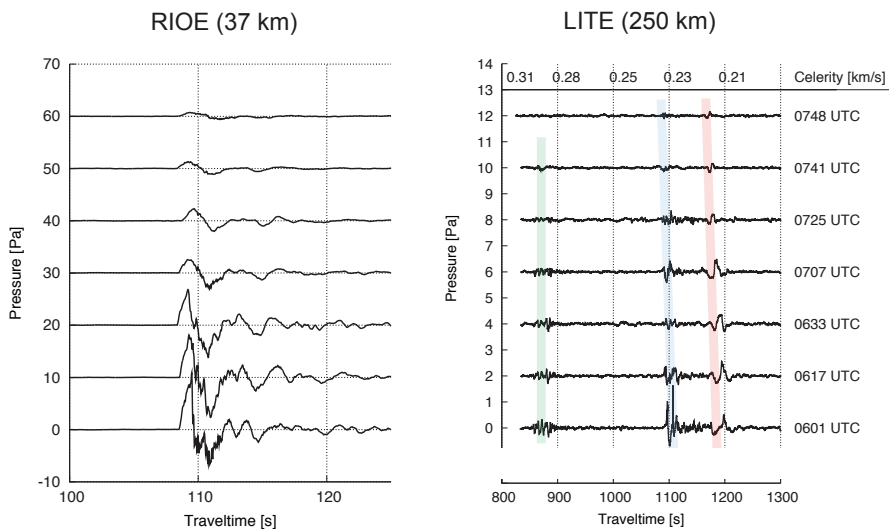

Fig. 1 Seven pairs of near-field (RIOE) and far-field (LITE) recordings of Mt. Tungurahua in Ecuador on 15 July 2006. Signals returning from the stratosphere, mesosphere and lower thermosphere are marked green, blue and red, respectively. The waveform structure and travel times (or celerity, defined as the distance between source and receiver divided by the travel time) have been used to infer properties of the wind and temperature at these altitudes, such as atmospheric tides (Assink et al, 2012, 2013) and gravity waves (Chunchuzov et al, 2015).

2 Background

2.1 The atmosphere as a waveguide

2.1.1 Relevant atmospheric parameters

Infrasound propagation is sensitive to temperature, wind and density (Brekhovskikh and Godin, 1999). Figure 2 shows a conceptual model of these quantities for a stratified atmosphere. The temperature and density profiles in Figure 2 are represented by polynomial fits to the US Standard Atmosphere (Lingevitch et al, 1999), the wind field is represented by a summation of sinusoids and Gaussian functions (Waxler et al, 2017).

The division of the atmosphere into the various layers is related to the vertical temperature gradient. Significant features of the horizontal wind fields include the jetstream around the tropopause, the circumpolar vortex (or 'stratospheric jet') around the stratopause and the atmospheric tides in the mesosphere and thermosphere. Generally, the zonal wind component is an order of magnitude larger than the meridional component. Vertical winds can typically be neglected for infrasound propagation, although these can be on the order of a few m/s in the mesosphere and thermosphere (Manson et al, 2002) and in deep convective regions of the troposphere. The exponential decrease in atmospheric density is due to the compressibility of air and the atmosphere's vertical extent.
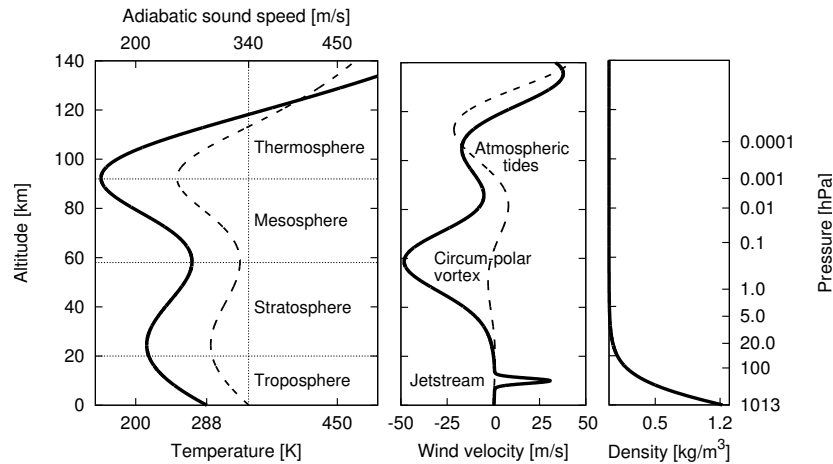

Fig. 2 A conceptual model of a boreal summer atmosphere's features at middle latitudes, based on the US Standard Atmosphere. Frames (a) through (c) show the absolute temperature (solid)/adiabatic sound speed (dashed), horizontal wind (zonal (W-E)–solid, meridional (S-N)–dashed) and density distribution up to 140 km altitude.

In reality, the atmosphere is more variable as a function of altitude, time, and geographical location. In particular, the discussed temperature and wind features show a much finer structure. Hourly global atmospheric specifications with a high spatial resolution up to $0.1°$ (or ~12 km) are currently available, e.g. through forecast systems of the European Centre for Medium-Range Weather Forecasts (ECMWF), the National Oceanic and Atmospheric Administration (NOAA) and the National Aeronautics and Space Administration (NASA). These models are mainly intended for medium-range forecasts on a global scale. An important aspect is that these models are hydrostatic, which implies that the vertical accelerations are considered to be small. Consequently, smaller-scale processes for which vertical motions are critical (e.g., deep convection and higher frequency gravity waves) are parameterised. Such processes can be better resolved in non-hydrostatic mesoscale models.

These higher resolution, mesoscale models (e.g., HIRLAM, HARMONIE and WRF) are designed for the purposes of short range weather forecasting on a more regional scale. Such models are nested and rely on global scale weather forecast models for the boundary conditions. HARMONIE and WRF are non-hydrostatic models, allowing for the computation of larger vertical velocities. These models are essential in the calculation of atmospheric gravity waves that lead to fine scale structure, which has a significant effect on infrasound propagation (Drob et al, 2013; Chunchuzov et al, 2015). Besides gravity waves, various other phenomena contribute to fine scale structure, including wind shear, Lee waves and extreme weather.

The vertical extent of the global forecast systems currently reaches up to mesospheric altitudes (typically, 0.01 hPa or ~80 km). However, the upper levels of the model, in the mesosphere, correspond to an absorptive sponge required for model stability. In addition, the models above the stratopause are currently unconstrained by data. The Ground-To-Space (G2S) model (Drob et al, 2003) combines the analysis products by NOAA and NASA with the Mass Spectrometer and Incoherent Scatter Radar (MSIS) (Picone et al, 2002) and Horizontal Wind Model (HWM) (Drob et al, 2008) climatologies in the upper mesosphere and thermosphere.

2.1.2 Atmospheric infrasound propagation

Infrasonic waves propagate in the atmosphere over large distances, in waveguides formed by the aforementioned temperature and wind speed variations and the Earth surface. Ground-to-ground propagation conditions are of particular interest given that most sources and receivers are ground-based, but similar concepts apply to elevated sources. Ducting is especially efficient in the tropospheric and stratospheric waveguides, because of geometrical spreading and absorption. Absorption is proportional to the acoustic frequency squared and inversely proportional to the ambient density. Hence, it is most significant in the mesosphere and lower thermosphere (Sutherland and Bass, 2004). The thermospheric waveguide is therefore most efficient for the lowest infrasonic frequencies, below 0.5 Hz. Another consequence of the lower density is that non-linear propagation effects (period lengthening and

wavefront steepening) become more significant at these altitudes. Period lengthening mitigates against signal attenuation (Lonzaga et al, 2015).

While the temperature structure forms the backbone of acoustic waveguides, (variations) in the winds are key in the determination of ducting conditions, in particular for the troposphere and stratosphere. In contrast to the lower thermosphere, the adiabatic sound speed around the tropopause and stratosphere is not sufficient to form a duct for ground-to-ground propagation, except at high latitudes where the troposphere can be sufficiently cold. Hence, tropospheric and stratospheric propagation paths predominantly exists in the direction of the jetstream and circumpolar vortex. In exceptional cases, bi-directional stratospheric ducting conditions may exist, for example during minor SSWs (Assink et al, 2014b).

The effective sound speed c_{eff} can be used to approximate to first order (Godin, 2002) the effects of temperature T and horizontal wind $\mathbf{w}_{uv}$ in the direction of propagation ϕ:

$$
\begin{aligned}
c_{\text{eff}}(z) &= \sqrt{\gamma R T(z)} + \left|\mathbf{w}_{uv}(z)\right| \cos\left(\phi - \phi_{\mathbf{w}_{uv}}(z)\right) \\
&= c_T(z) + w_a(z)
\end{aligned}
\tag{1}
$$

Here, $\gamma = 1.4$ and $R = 286.9\,\mathrm{J\,kg^{-1}\,K^{-1}}$ are the ratio of specific heats and the specific gas constant for dry air, respectively. Note, that both propagation azimuth ϕ and wind direction $\phi_{\mathbf{w}_{uv}}$ are clockwise relative to the North. The orientation of the source and receiver locations determine the propagation azimuth ϕ. This angle is used to estimate the along-track wind (w_a) and cross-wind (w_c) components, by ro-
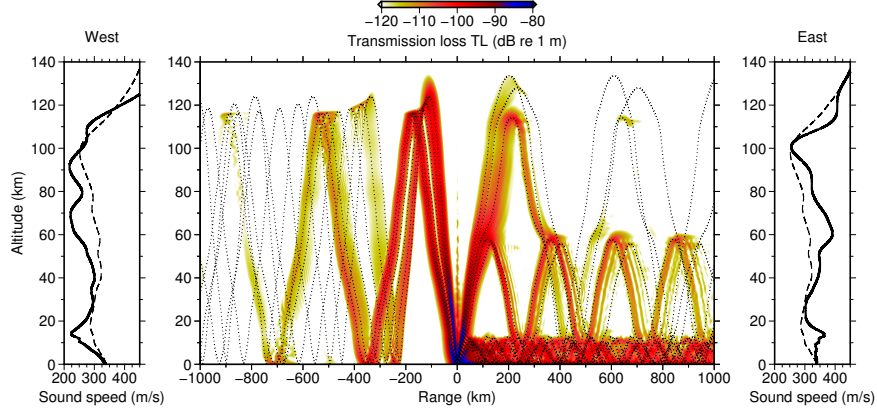

Fig. 3 Typical infrasound propagation conditions during the boreal winter. Effective sound speed profiles are shown on the sides with bold lines. The dashed curves in the center frame show the ray paths, dark colors indicate presence of acoustic energy at 0.5 Hz. Towards the west infrasound propagates in the thermospheric waveguide, towards the east infrasound propagates in the tropospheric, stratospheric and thermospheric waveguides. Acoustic energy in the thermosphere is strongly attenuated, as indicated by the lighter colors with range.

tating the zonal (w_u) and meridional (w_v) components of the horizontal wind vector $\mathbf{w}_{uv}$.

$$\begin{pmatrix} w_a \\ w_c \end{pmatrix} = \begin{pmatrix} \sin\phi & \cos\phi \\ -\cos\phi & \sin\phi \end{pmatrix} \begin{pmatrix} w_u \\ w_v \end{pmatrix} \tag{2}$$

An example of infrasound propagating from a point source positioned on the ground at 0.5 Hz is shown in Figure 3. The atmospheric model is somewhat typical of the boreal winter at mid-latitudes (20 to 60 °N) and features a strong jet-stream around 13 km and a circumpolar vortex around 60 km altitude. Zones of audibility are colored and represent the full-wave solution obtained by the method of normal modes (Waxler et al, 2017; Assink et al, 2017); the dashed lines (rays) are approximately perpendicular to the wavefronts. Regions without significant acoustic energy are so-called 'zones of silence'. In reality, the zones of silence are filled in, for example, by scattering off small-scale structure (e.g. Chunchuzov et al, 2015).

The atmosphere is a highly dynamical medium, which leads to varying propagation characteristics around the globe (Le Pichon et al, 2005; Assink et al, 2014a). A consequence is that recorded infrasonic waveforms for repeated experiments vary drastically (Kulichkov, 2010). In contrast, seismic arrivals tend to be relatively invariant over time. This suggests that the variability in the infrasonic waveforms can be used to monitor atmospheric variability, especially in combination with seismic data from the same source. Gibbons et al (2015) have analysed repetitive seismo-acoustic sources in northern Scandinavia for this purpose. Donn and Rind (1972) used observations of signals from ocean wave interactions on seismic and infrasound stations (respectively microseisms and microbaroms) to monitor winds in the stratopause and lower thermosphere.

A more detailed discussion of infrasound propagation can be found in the chapter by Waxler and Assink (this volume).

2.2 Relating wind and temperature to infrasound wavefront parameters

Consider a vertical plane through the atmosphere, intersecting source and receiver. As the atmosphere is predominantly a stratified medium, the in-plane and out-of-plane atmospheric quantities (respectively T, w_a and w_c) each have a specific influence on infrasound wavefront parameters. The former largely determine the vertical refraction along a great-circle path through vertical variations in sound speed and wind. This has an effect on the travel time (e.g., Assink et al, 2012) - as travel time and sound speed are directly related - as well as the trace velocity. The cross-winds control the out-of-plane propagation effects. This is measured as the deviation from the theoretical azimuth at a distant infrasound array.

The azimuth deviation due to cross-wind w_c is illustrated in Figure 4c, as the angle between the true azimuth (gray line) and the propagation azimuth (purple line) needed to arrive at the receiver location. Note that the propagation path is

denoted by the dashed red line. At the receiver location, the observed back azimuth (orange line) does not point towards the source. Only in the hypothetical case of zero cross-wind, all four mentioned lines would align (e.g. Smets et al, 2016).

The trace velocity c_{trc} is the inverse of the horizontal projection of the slowness vector (defined as the inverse of the propagation velocity vector) and describes the horizontal propagation speed of a ray with grazing angle θ as $c_{trc} = \frac{c_{eff}}{\cos\theta}$. For a ray in a layered medium, trace velocity is invariant and is necessarily equal to or larger than the effective sound speed in that layer. At a ray's turning point (or return height), $\theta = 0°$, and the trace velocity equals the effective sound speed at the return height, as illustrated in Figure 5. This relationship allows for an immediate identification of return heights with associated (wide) range of trace velocities from an effective sound speed profile (Rind et al, 1973; Assink et al, 2014a; Bertin et al, 2014).

Thus, a complementary set of infrasound wavefront parameters exist that is sensitive to temperature and horizontal wind. Since these parameters can be determined using array processing techniques (e.g., Melton and Bailey (1957); Smart and Flinn (1971); Cansi (1995); Szuberla and Olson (2004)), one could then invert for wind and temperature in the atmosphere. In Section 3, methods are discussed that rely on ray theory. Inversion methods that use the full waveform to invert for small-scale atmospheric structure can be found in the chapter by Chunchuzov et al. (this volume).
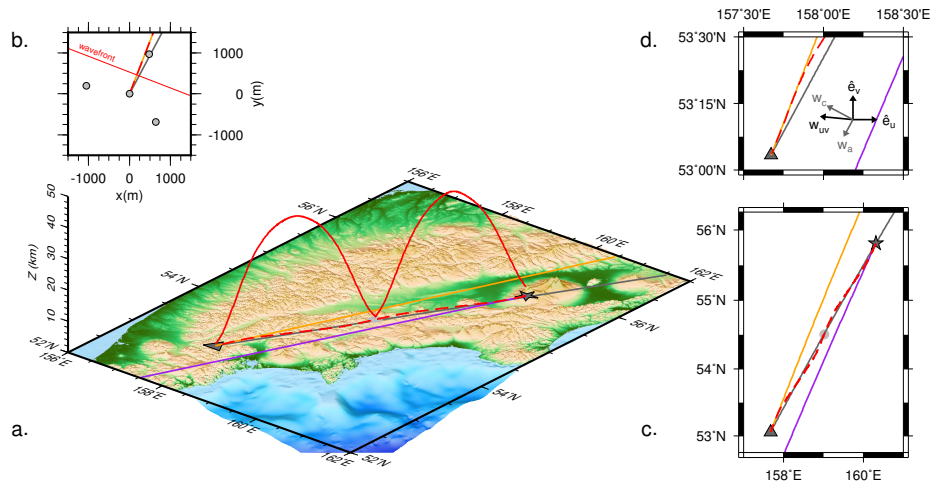

Fig. 4 (a) Map of the Kamchatka peninsula in Russian Federation (55.8 ° N, 160.3 ° E), (b) IMS array IS44 elements layout (triangles) with theoretical, observed and ray simulated back azimuth angles, all with respect to the array central element. The thin red line perpendicular to the observed back azimuth indicates the incoming planar wavefront. (c) Horizontal projection (top-view) of (a) with the gray circle indicating the reflection at the ground. (d) Zoom in on (c), showing the receiver area with the observed and theoretical back azimuth angles. Figure adapted from Smets et al (2016).

2.2.1 The temporal variation of infrasound observations

As a consequence of the relation between atmospheric wind and temperature and infrasound wavefront parameters, temporal variations in these quantities will also be reflected in the infrasonic recordings. This illustrates the sensitivity of infrasound parameters to the upper atmosphere. Variations in upper atmospheric winds and temperatures with timescales ranging from (multi-)annual to hourly can in principle be identified by analysing array processing results. In reality, matters can be complex due to complexities in infrasonic source characteristics, propagation paths and adverse local wind noise conditions that may hamper detection.

Various insightful results have been obtained with the analysis of steady and impulsive infrasound sources, in particular explosions (Kulichkov, 2010) and volcanoes (Le Pichon et al, 2005; Antier et al, 2007; Assink et al, 2012), which have the advantage that the source location, timing and frequency content are often well constrained (cf., Figure 1). However, the sparsity of these sources lead to a need for a more ubiquitous and continuous source. Thanks to advances in microbarom source modeling (Waxler and Gilbert, 2006), microbaroms become more and more in reach for atmospheric remote sensing (Smets and Evers, 2014; Assink et al, 2014b).

The ratio of effective sound speed around the stratopause versus the ground (the effective sound speed ratio), controls to first approximation where ground to ground infrasound detections can be expected since ray-theoretic ground returns require a sound speed greater than or equal to that on the ground (Figure 6). The circumpolar vortex determines to a large extent the effective sound speed around the stratopause. On a global scale, it was shown that the general trend in microbarom signal back-azimuth recorded on the IMS network is consistent with the seasonal reversal of the circumpolar vortex (Figure 7) (Garcés et al, 2004; Landès et al, 2012).

At shorter time scales, changes in the direction and intensity of the polar vortex determine the sensitivity of the arrays for sources located in specific directions. In particular, several studies have focused on the sensitivity to both minor (Assink et al, 2014b) and major (Donn and Rind, 1972; Evers and Siegmund, 2009; Smets and Evers, 2014) SSW events. The study of SSW events, that constitute the most
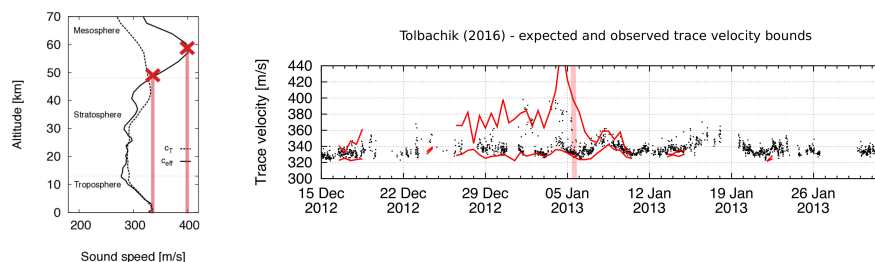

Fig. 5 In a layered medium, the minimum and maximum expected trace velocity can be estimated from an effective sound speed profile. This implies that trace velocity bounds can be used to estimate the return heights and corresponding sound speeds aloft.

dramatic dynamics in the stratosphere, is of particular interest given the associated impact on the lower atmosphere (e.g. Lee et al. (this volume)). The study of SSWs using infrasound is further discussed in the chapter by Smets et al. (this volume).

3 Inverse methods for upper atmospheric temperature and wind

The objective is to estimate the atmospheric wind and temperature profiles that explain ground-based infrasound observables. Infrasound wave front parameters recorded at infrasound arrays are used as input parameters. A representation of the profiles with a limited number of parameters ('model parameterization') is necessary, given the finite number of observables. This will be discussed in the following subsection. The forward problem describes how observables $\mathbf{d}$ and model parameters $\mathbf{m}$ are related through function $\mathbf{G}$:

$$\mathbf{d} = \mathbf{G}(\mathbf{m}) + \boldsymbol{\varepsilon} \tag{3}$$
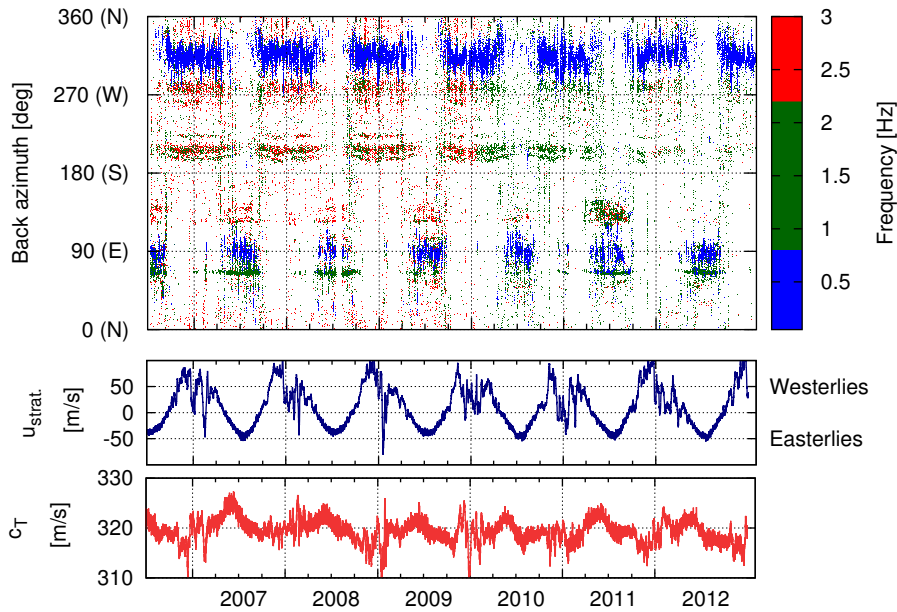
Fig. 6 Comparison of the stratospheric mean zonal wind and adiabatic sound speed with infrasound observations at CTBTO station IS48 in Tunisia ($36°$ N). The zonal wind and sound speed are averaged between 5.0 and 0.2 hPa (resp. 36 and 60 km) and show the annual circulation of the circumpolar vortex including the sudden variations that are related to SSWs. The detectability of infrasound from a specific direction is related to stratospheric propagation conditions, that are largely influenced by the zonal wind.

Here, $\mathbf{G}$ and ε correspond to wave propagation (e.g. ray theory) and an error term, respectively. Thus, one is to solve the inverse to Equation 3, thereby minimizing term ε. If the forward problem can be linearized, Equation 3 can be written in the form of $\mathbf{d} = \mathbf{Gm} + \boldsymbol{\varepsilon}$ (e.g., Tarantola, 2005).

The inverse problem is similar to the seismic tomography problem. This non-linear inverse problem is ill-posed and therefore non-unique solutions exist. The non-uniqueness may arise due to approximations in the propagation theory (e.g. geometrical acoustics), model parameterizations, as well as the incomplete sampling of the atmosphere leading to some model parameters being better constrained by the data than others. Therefore, regularization of data and model spaces using apriori information and model appraisal are essential. A common regularization in inverse methods is Tikhonov regularization, which is a statistical regularization based on the covariance of both noise and model parameters (e.g., Snieder and Trampert, 1999; Tarantola, 2005).

All of the presented inversion methods throughout this Section assume a stratified atmosphere. This is a reasonable approximation for propagation paths over regional distances (e.g., on the order of hundreds of kilometers). Consequently, these inversion methods can be used to invert for 1-D upper atmospheric structure in the
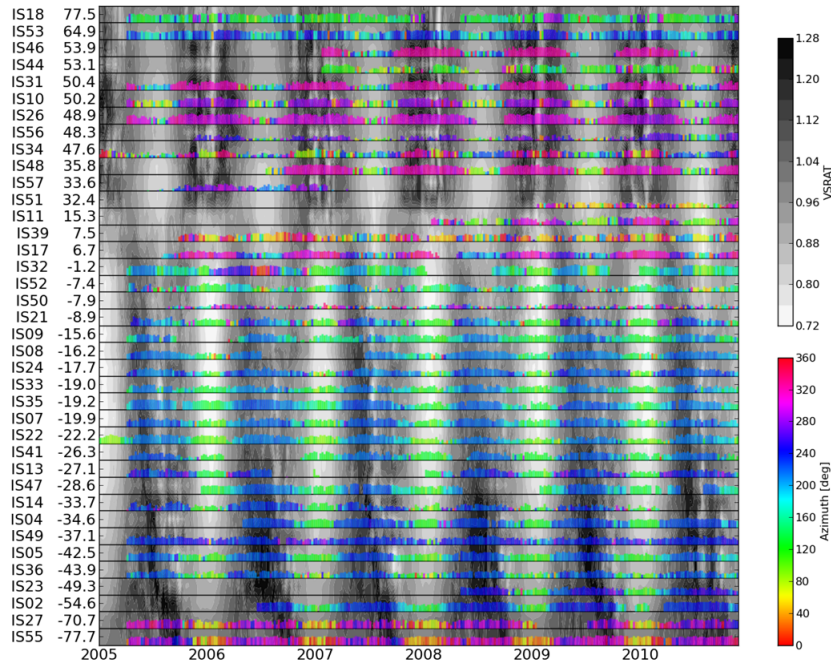

Fig. 7 Similar to Figure 6, pointing out the trend in infrasound observations and seasons on a global scale. There is a clear relation to the effective sound speed ratio (VSRAT). Figure adapted from Landès et al (2012).

vicinity of the infrasound array, although most of the sensitivity is confined to the re-
fracting altitudes. On going research efforts focus on the potential application of in-
frasound assimilation in NWP models. This requires a more global scale approach.
A first step towards this is the evaluation of weather forecasts using infrasound,
which is described in Section 4.

3.1 Parameterization of atmospheric profiles

In earlier studies, ad-hoc solutions have been considered as parameterizations, such
as Gaussian correction factors (Le Pichon et al, 2005). Drob et al (2010) proposed
principal component analysis (PCA) as parameterization method for infrasonic in-
version studies. PCA allows for an efficient and appropriate description of the
spatio-temporal variability of atmospheric profiles with a limited degrees of free-
dom in the inversion. Various authors have since then adopted this method (e.g., La-
lande et al, 2012; Assink et al, 2013; Arrowsmith et al, 2013; Lonzaga et al, 2015).
Using PCA, de-meaned temperature and wind profiles (e.g., from ECMWF or G2S)
are decomposed into a set of orthogonal functions, each scaled by a time-dependent
coefficient. The original profiles can be recovered by evaluation of a sum:

$$\mathbf{m}(t,z) \approx \bar{\mathbf{m}}(z) + \sum_{n=1}^{N} \beta_n(t)\psi_n(z) \tag{4}$$
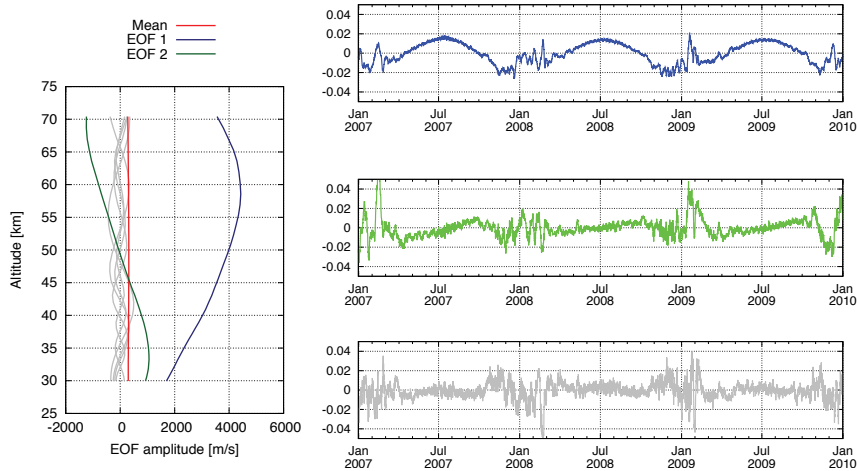

Fig. 8 Emperical Orthogonal Function (EOF) parameterization of three years of effective sound
speed profiles between 30 and 70 km altitude for propagation from Mt. Etna to station IS48. The
wind and temperature profiles are retrieved from ECMWF analysis. Most of the variance is de-
scribed by two EOFs of the lowest order, with the higher order EOFs describing finer structure.
The associated EOF coefficients are shown to the right. Figure adapted from (Assink et al, 2014a).

where $\bar{\mathbf{m}}(z), \beta_n$ and ψ_n represent the time-averaged profile, the model parameters and the EOFs, respectively. Wind and temperature profiles can be approximated by a limited number of terms (Drob et al, 2010). Truncation is not necessary, since the EOFs are orthogonal and can be constructed to be sensitive to specific regions. Thus, the inverse problem is reduced to the estimation of (specific) model coefficients β_n (Assink et al, 2013; Lonzaga et al, 2015).

Infrasound propagation is sensitive to temperature and wind, which are dynamically linked through the equations of fluid dynamics. The thermal wind relation can be used to relate temperature and wind gradients in atmospheric regions where the geostrophic and hydrostatic balance applies (Andrews et al, 1987). This implies that formally temperature and wind cannot be treated independently in an inversion. In a first approach, it is assumed that the variations in wind are much larger than those in the temperature (Le Pichon et al, 2005; Drob et al, 2010; Lalande et al, 2012; Assink et al, 2013; Arrowsmith et al, 2013).

Alternatively, assuming an effective sound speed for a specific propagation azimuth, one can invert for an effective sound speed profile, taking the combined effects of wind and temperature into account. This is done by parameterizing a time-series of effective sound speed profiles (Figure 8) and modifying the effective sound speed EOF coefficients in the inversion procedure (Assink et al, 2014a).

Note that the imposed model parameterization imposes some form of regularization on the inversion. Using PCA, the inversion result will be constructed from the Emperical Orthogonal Functions (EOFs) that are generated from the apriori models. For example, temperature and wind features will large vertical gradients are not represented as these are not present in NWP models. The retrieval of such features, by considering partially reflected arrivals that reflect off these features is discussed in Chunchuzov et al. (this volume).

3.2 Solving the inverse problem

The solution of the inverse to Equation 3, depends on the relation $\mathbf{G}$ between $\mathbf{d}$ and $\mathbf{m}$. For linear problems the resulting system of equations are straightforward to solve. Weakly non-linear problems can be solved by iterative methods based on linearisation, such as the Levenberg-Marquardt method. For strongly non-linear problems in which local minima in model/data misfit are to be expected the model space search is more involved. Various methods have been applied to solve the infrasonic inverse problem, including linearization (Lalande et al, 2012), non-linear optimization (Le Pichon et al, 2005; Drob et al, 2010; Arrowsmith et al, 2013) and grid search methods (Assink et al, 2013). Current research focuses on the application of Monte Carlo methods that sample larger model spaces more efficiently (Sambridge and Mosegaard, 2002).

3.2.1 Linearized inversion

Lalande et al (2012) have proposed an inverse method approach based on the linearization of geometrical acoustics operator **G**. This approach relies on Fermat's principle to linearly relate perturbations in travel time to perturbations in medium velocity along a reference ray. This is valid for small velocity perturbations only as the ray position is dependent on the medium velocity. The forward problem is treated in the high-frequency approximation using the Hamiltonian formulation where the complete first-order ray perturbation theory is developed in order to construct the Fréchet derivative matrix. An iterative conjugate gradient method is used to minimize the objective function. The model space is parameterized using EOFs. The choice of a starting model is a critical step since it should be located in the
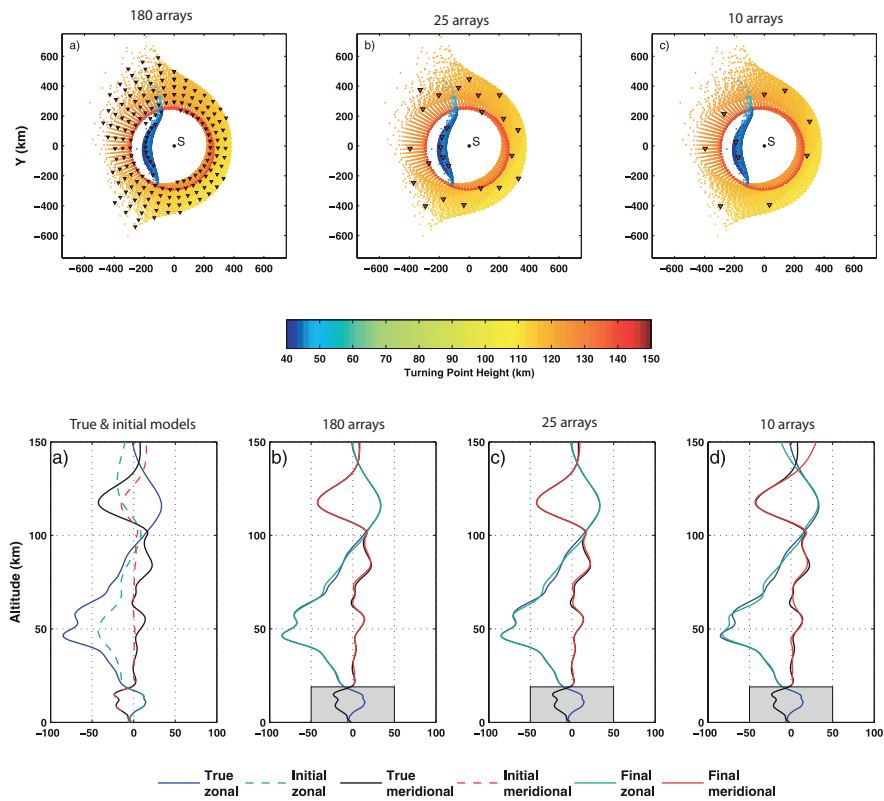

Fig. 9 Linearized inversion results obtained by the method of Lalande et al (2012). Infrasound wavefront parameters are generated using ray theory and the wind profiles (solid lines, lower left frame). A subset of these points are sampled and used to invert for the wind model, using a different initial profile (dashed line, lower left frame). In all cases, the true modal is retrieved.

vicinity of the global minimum. In principle, model appraisal is feasible with iterative least-squares formalisms (Trampert and Leveque, 1990).

Figure 9 shows example inversion results for the synthetic data set computed with NRL-G2S specifications for boreal summer conditions. For these relatively smooth wind profiles, without much fine vertical structure, the inversion works reasonably well as the original profiles are recovered successfully.

3.2.2 Non-linear optimization methods

The study by Le Pichon et al (2005) was the first one in the estimation upper atmospheric updates from actual infrasound data. Corrections to G2S profiles were found by correcting for unexplained observations of back-azimuth values from a volcano, using a non-linear optimization package.

This approach was further developed by Drob et al (2010), solving Equation 3 as a weighted orthogonal distance regression problem, in order to handle uncertainties
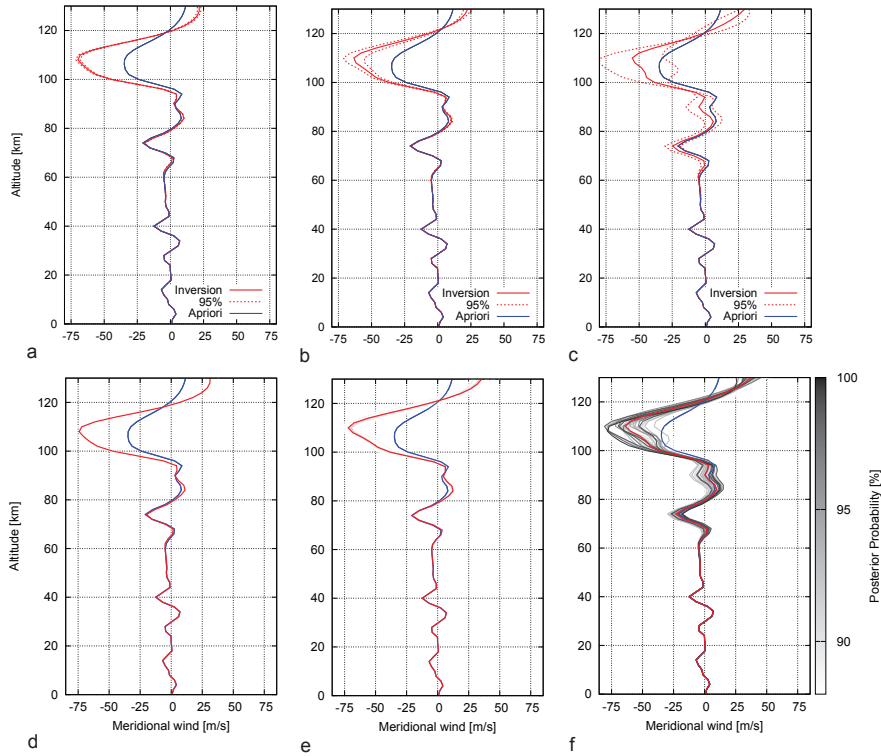

Fig. 10 Comparison of the methods described by Drob et al (2010) and Assink et al (2013) for a inversion case in which (a-d) two, (b-e) three and (c-f) four EOF parameters are adjusted.

in the data and model spaces. A software package (Zwolak et al, 2005) is used
to solve the regression problem and estimate a number of EOF parameters. The
objective function is iteratively approximated within a trust-region to find an update
to the initial parameter guess. The Jacobian matrix, required to find next iteration, is
approximated using finite-differences. As with the linearized inversion method by
Lalande et al (2012), the algorithm is sensitive to local minima. The method uses
the derivatives around the final solution to compute the 95% confidence intervals.

Arrowsmith et al (2013) and Blom and Marcillo (2017) have extended the method
to estimate stratospheric wind speeds from non-ground truth events using a network
of infrasound arrays. In this approach, the celerity of a unique ray path (ducted
in the stratosphere) is estimated from measurements made at distances covering a
full stratospheric bounce (between 150-250 km). The estimated celerity is used to
identify perturbations to an initial atmospheric specification that improve agreement
between observed and predicted celerities.

Although the search algorithm allows for a quick search and provides uncertainty
estimates, it is not clear how well the algorithm can deal with non-linearities in the
objective function. Figure 10 shows a comparison between the optimization algo-
rithm and a grid search (see next subsection). Although the methods compare well,
more studies are required to see towards which extent such an approach can be used,
for example for cases for which non-linearities due to interaction between different
acoustic ducts becomes significant (Lalande et al, 2012).

3.2.3 Direct search methods

In some cases, direct search methods are the only option to search the model space
for potential solutions due to non-linearities in the objective functions. Large pop-
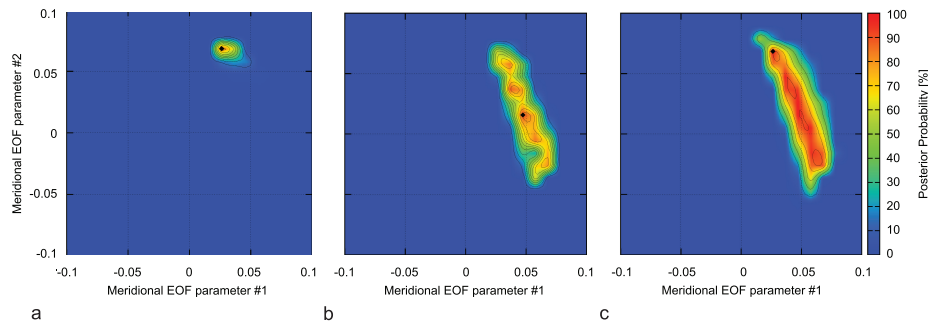ulations of models can be generated, e.g. using Monte Carlo techniques or grid

Fig. 11 Posterior probability for an inversion using a grid search where respectively (a) two, (b)
three and (c) four parameters are varied. The uncertainty in traveltime and trace velocity are 1 s and
5 m s^{-1}, respectively. The addition of parameters to the search broadens the posterior distribution,
as expected from the stochastic formulation. Figure adapted from Assink et al (2013).

searches if the model space is not too large (which is the case for specific problems). Generating populations can be computationally demanding, especially when the theory is numerically involved or the dimensionality of the model space is large.

The advantage of direct search methods is that uncertainty analyses are easily incorporated. Grid searches in combination with Bayesian statistics have been used for the solution of thermospheric (Assink et al, 2013) and stratospheric (Assink et al, 2014a) inverse problems, allowing for an assessment of the posterior uncertainties. Posterior distributions σ are determined from the apriori model space $\rho(\mathbf{m})$ distribution and the likelihood function L (Tarantola, 2005):

$$\sigma(\mathbf{m}|\mathbf{d}) \propto \rho(\mathbf{m})L(\mathbf{m},\mathbf{d}) \tag{5}$$

Both the likelihood function L and apriori model space $\rho(\mathbf{m})$ can be represented by a Gaussian probability density function (pdf). $\rho(\mathbf{m})$ expresses the likelihood of a model given apriori values and associated uncertainties, while L expresses how well the observations are predicted:

$$\rho(\mathbf{m}) = e^{-\frac{1}{2}\left[\left(\mathbf{m}(z)-\mathbf{m}_{\text{prior}}(z)\right)^T \mathbb{C}_M^{-2}\left(\mathbf{m}(z)-\mathbf{m}_{\text{prior}}(z)\right)\right]} \tag{6}$$

$$L(\mathbf{m},\mathbf{d}) = e^{-\frac{1}{2}\left[(\mathbf{G}(\mathbf{m})-\mathbf{d})^T \mathbb{C}_D^{-2}(\mathbf{G}(\mathbf{m})-\mathbf{d})\right]} \tag{7}$$

Here, the $\mathbb{C}_M$ and $\mathbb{C}_D$ covariance matrices describe uncertainties in model and data space. Typically, uncertainties between observations and model parameters are assumed to be uncorrelated, reducing $\mathbb{C}_M$ and $\mathbb{C}_D$ to diagonal matrices describing variances. When using PCA, β replaces $\mathbf{m}$ in the aforementioned equations.
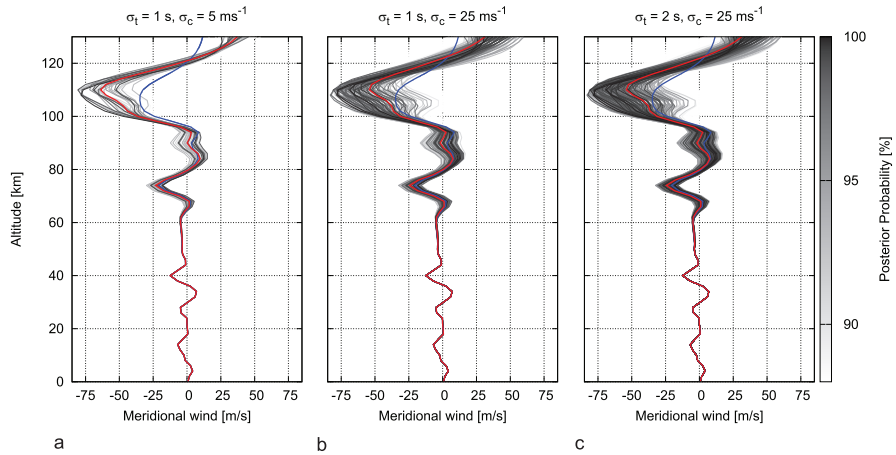

Fig. 12 Meridional wind profiles obtained from the posterior model distribution, for different choices of observational uncertainties. The model space is given by a uniform distribution centered within 50 m s^{-1} of the prior model. Figure adapted from Assink et al (2013).

Figure 11 shows the posterior distributions for a grid search using volcanic infrasound data (Assink et al, 2013), where respectively (a) two, (b) three and (c) four EOF parameters of the meridional wind field are adjusted, while others are kept fixed. It can be seen that the addition of parameters to the search leads to (1) an increase of posterior probability and (2) a broadening of the posterior distribution. This is consistent with the formulation of the posterior model as a linear combination of stochastic variables. As expected, the posterior distribution also broadens when the observational uncertainty is increased (Figure 12).

Another example of such an Bayesian inversion is presented in Figure 13. The Figure shows a comparison of infrasound parameters associated with Mt. Etna (black) with simulations using ECMWF profiles for the year 2008. Differences in observations and predictions of trace velocity (e.g., at the blue arrow) are used as an input for the inversion procedure for effective sound speed profiles (Assink et al, 2014a). An EOF parameterization (Figure 8) is used to parameterize the model space. An example inversion for 2 October 2008 is shown on the right of Figure 13 and suggests that during equinox periods, the effective sound speed profiles are underestimated.
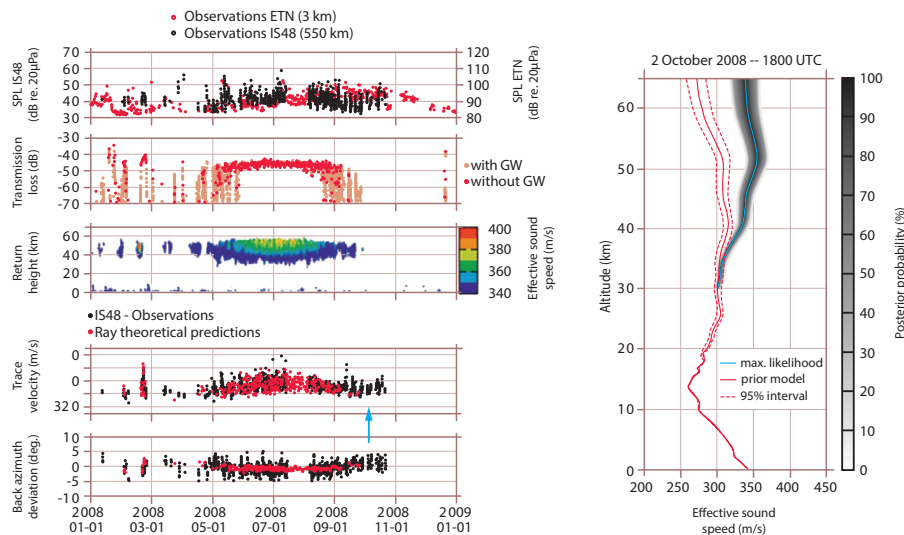

Fig. 13 Left: the two lower frames compare the predicted variations (red dots) with the observations (black dots). The middle frame shows the possible return heights of infrasound with the associated effective sound speed values. The two upper frames show the sound pressure levels near the source and receiver and the calculated transmission losses, respectively. The transmission losses are calculated using an ensemble of atmospheric profiles with gravity wave realizations.
Right: an example Bayesian inversion of the effective sound velocity profiles for 2 October 2008 (blue arrow, left subfigure). The dotted red lines indicate the estimated 95% uncertainty interval around the apriori model state. The gray area corresponds to the posterior distribution of retrieved effective sound speeds. The maximum likelihood profile is represented by a solid cyan line. Figure adapted from Assink et al (2014a).

4 Towards assimilation in numerical weather prediction models

While significant progress has been made in the development of infrasonic remote sensing methods, the approaches are limited to inversions for 1-D atmospheric structure on a local scale. It is also important to realize that the scales of interest of atmospheric variability are different for infrasound monitoring and NWP modeling applications (Le Pichon et al, 2015). Thus, it may be of interest for the infrasound community to estimate upper atmospheric wind and temperature corrections for the precise modelling of infrasound arrivals (e.g. for explosion yield estimation) (Assink et al, 2013; Lonzaga et al, 2015).

However, for the assimilation of infrasound data in NWP models, there is a need to develop techniques on a more global scale. Instead of inverting observations to atmospheric properties, an useful approach could be with the forward simulation of infrasound observables from NWP models, to be compared with global infrasound observations. Thus, rather than extracting atmospheric specification at one specific point in time and space with high detail, it might be more suitable to feed the assimilation with path integrated specifications. Such an approach would help to overcome current limitations (e.g., 1-D, uncoupled temperature and wind) and would be in line with existing assimilation strategy (e.g., 4D-Var). Moreover, the approach has already been applied to similar remote sensing techniques such as GPS Radio Occultation for the estimation of temperature. Such an effort should be carried in close collaboration with the NWP community; this has been one of the goals of the
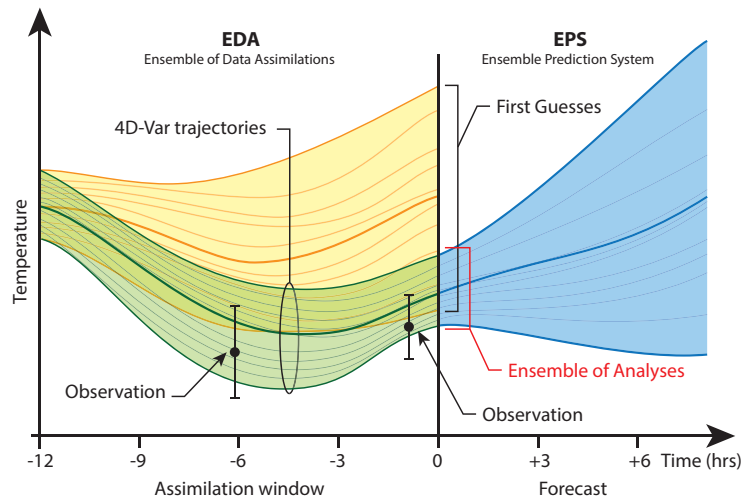

Fig. 14 Figure by ECMWF. Schematic overview showing the ensemble of data assimilation and prediction systems, such as used by NWP centers. Infrasound could be used to constrain which members of the ensemble are more likely than others. EDA and EPS are ECMWF products.

Atmospheric dynamics Research InfraStructure in Europe (ARISE) projects (Smets et al, 2014).

Before this effort is realized, infrasound data already represents a valuable resource to evaluate NWP models and help select which forecast members are more likely than others (Figure 14 and 15). This shift in focus has lead to research on the evaluation of analyses (Assink et al, 2014a), ensemble members (Smets et al, 2015) as well as forecasts (Smets et al, 2016). In particular evaluations of SSW events, during which significant stratosphere-troposphere coupling may occur (Charlton and Polvani, 2007), is of direct interest to the NWP community because the skills of NWP models in the stratosphere are then challenged.

5 Interferometric techniques for atmospheric infrasound

In the majority of the studies that have previously been discussed, signals from steady (either transient or quasi-continuous) infrasound sources have been used. Notable examples are anthropogenic (accidental) explosions and volcanoes. Such sources, however, are relatively sparse. Because of its ubiquitous nature, micro-
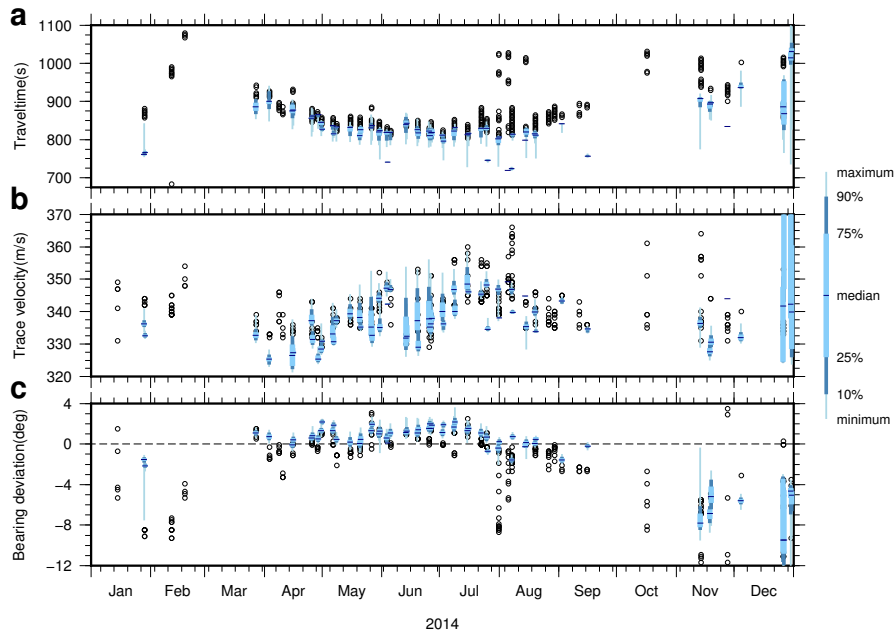

Fig. 15 Evaluation of a ensemble of analyses (see Figure 14) using infrasound recordings of mine explosions (black dots). For each simulated event the percentile distribution (blue) indicates the minimum, 10th centile, 25th centile, median, 75th centile, 90th centile, and the maximum value. Figure adapted from Smets et al (2015).

baroms are a viable alternative for atmospheric imaging purposes. For example, both major (Evers and Siegmund, 2009; Smets and Evers, 2014) and minor (Assink et al, 2014b) SSW events have been detected using microbaroms. In addition, advances in microbarom source modeling (Waxler and Gilbert, 2006, e.g.) may aid such applications.

The ubiquitous nature of the microbaroms fosters the development of infrasonic remote sensing methods that can be applied to such type of coherent noise. For that purpose, so-called interferometric techniques are of particular interest. Applied to acoustic wavefields, interferometry refers to the principle of generating new acoustic responses from existing wavefields. By cross-correlating pressure fluctuations recorded by a pair of receivers, the medium's Green's function between the locations of those two receivers can be retrieved (e.g., Lobkis and Weaver, 2001; Wapenaar and Fokkema, 2006). In case of illumination by transient sources, an explicit summation over sources is required. Application to noise sources, however, renders this summation unnecessary. Instead, crosscorrelations need to be averaged over a large amount of time (e.g., Godin et al, 2010; Weemstra et al, 2012). As such, the lack of correlation of the noise sources is exploited (Wapenaar and Fokkema, 2006; Seats et al, 2012).
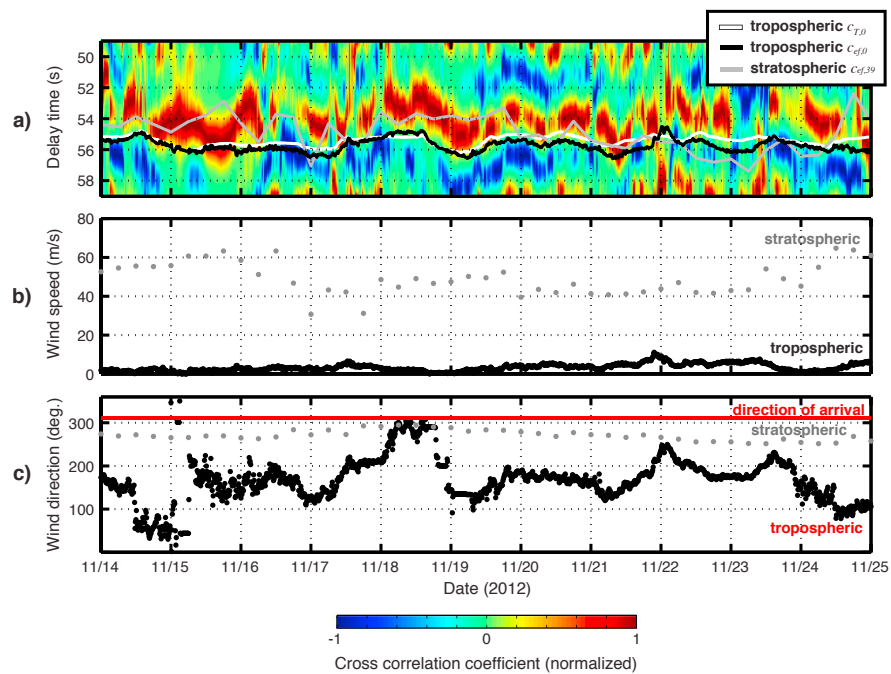

Fig. 16 Application of infrasonic interferometry to estimate tropospheric effective sound speed conditions. Figure adapted from Fricke et al (2014).

The relation between the time-averaged crosscorrelation and the Green's function is only exact under specific conditions. The two most notable conditions are (i) a uniform illumination of the medium and (ii) the absence of dissipation (Wapenaar and Fokkema, 2006). In practice, the violation of these conditions implies that only an estimate of that Green's function is retrieved (e.g., Weemstra et al, 2015). Nevertheless, as long as sufficient sources are present in the so-called stationary-phase directions (Snieder, 2004), the retrieved Green's function estimate is sufficiently accurate to be exploited. Sources need only to be in the Fresnel zone to retrieve the stationary phase. For most interferometric applications, the medium parameters are assumed to be time-invariant. Implicitly, these applications rely on a so-called correlation-type reciprocity theorem (Wapenaar and Fokkema, 2006). The first successful application of interferometry using microseisms (the seismic counterpart of microbaroms) is due to Shapiro and Campillo (2004). Interferometry has also been applied to other media and/or in other contexts: for example, helioseismology (Duvall et al, 1993), underwater acoustics (Roux and Kuperman, 2004; Evers et al, 2017) and ultrasonics (Weaver and Lobkis, 2001).

Infrasonic interferometry is based on the theory of nonreciprocal Green's function retrieval (Wapenaar and Fokkema, 2006; Godin, 2006). Nonreciprocity, due to the anisotropic propagation by wind, is overcome by reversing the horizontal wind for propagation in opposite directions. This holds for a laminar flow with a constant wind velocity. Once the delay time between two stations is found, it can be used to retrieve wind and temperature conditions (e.g., Marcillo and Johnson, 2010; Godin, 2014). In contrast to seismology, the averaging time is much shorter for infrasonic interferometry as the variability of the medium is on much smaller time scales.

Both Haney (2009) and Fricke et al (2014) have demonstrated that it is possible to apply interferometry to tropospherically propagating microbarom signals that are in the stationary-phase direction. Thus, it is possible to estimate the changes of the tropospheric sound speed and the wind speed nearly continuously in time (Figure 16). Infrasound produced by wind turbines, which can propagate tens of kilometers in tropospheric ducts is another source of quasi-continuous noise with the potential to be used for interferometric studies in the lower atmosphere (Marcillo et al, 2015; Pilger and Ceranna, 2017). Coda wave interferometry (Snieder, 2006) can also be applied to acoustic waveforms from the same source-sensor pair (assuming a discrete repeating source) to estimate changes in atmospheric conditions. Small time delays between similar features in the waveforms (relative to the signals' onset) are extracted and modeled as bulk changes in air temperature (Marcillo et al, 2014). An example of coda wave interferometry is shown in Figure 17.

As such, the technique is useful for the evaluation of weather models near the ground surface, for example in the atmospheric boundary layer. This is of particular interest in regions with a limited number of in-situ observations, e.g. over sea and around the equator. Stratospheric propagation between receiver pairs requires longer propagation distances and traveltimes, hence both the required period of constant illumination and the required time-length of stationarity of the atmosphere increase. The application of this technique to stratospherically propagating signals thererfore remains a challenge for the future.

6 Conclusions

The sensitivity of infrasound to atmospheric temperature and wind, the ability to propagate over large horizontal distances through the middle and upper atmosphere and the presence of a global infrasound network make that infrasound is an interesting technique for atmospheric remote sensing. Over the recent years, significant progress has been made in the development of infrasonic remote sensing methods for the estimation of 1-D atmospheric structure. The developed methods range from linearized inversions to direct search methods. Current research focuses on the application of methods that sample larger model spaces more efficiently and interferometric techniques for atmospheric infrasound.

For the assimilation of infrasound data in NWP models, there is a need to develop techniques on a more global scale. Instead of inverting observations to atmospheric properties, an useful approach could be with the forward simulation of infrasound observables from NWP models, to be compared with global infrasound observations. Such an approach would be compatible with existing assimilation strategies. Application of this method in the evaluation of NWP weather products (ensembles of analyses, forecasts, climatologies) shows the added value of infrasound, e.g. during SSWs and equinox periods.
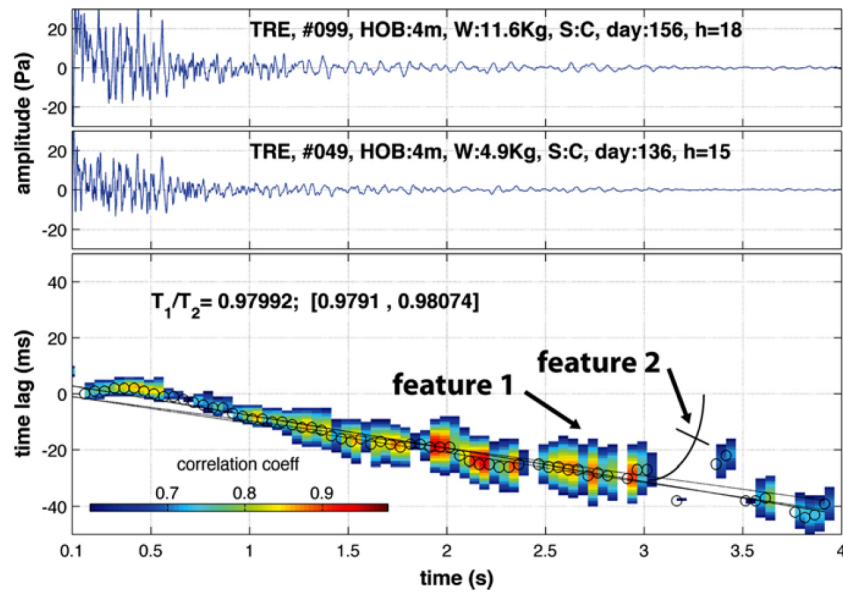

Fig. 17 The upper panels show the acoustic coda from two explosions (with different charge sizes) recorded at the same location 20 days apart. The lower panel shows the corresponding cross-correlogram (XC). Feature 2 in the XC is modeled as a variation in bulk air temperature that produces a small change in effective velocity. Adapted from Marcillo et al (2014).

References

Andrews DG, Holton JR, Leovy CB (1987) Middle atmosphere dynamics. Academic Press, 1st edition

Antier K, Le Pichon A, Vergniolle S, Zielinski C, Lardy M (2007) Multiyear validation of the NRL-G2S wind fields using infrasound from Yasur. Journal of Geophysical Research 112(D23110), DOI 10.1029/2007JD008462

Arrowsmith S, Marcillo O, Drob DP (2013) A framework for estimating stratospheric wind speeds from unknown sources and application to the 2010 december 25 bolide. Geophysical Journal International 195(1), DOI 10.1093/gji/ggt228

Assink J, Waxler R, Frazier W, Lonzaga J (2013) The estimation of upper atmospheric wind model updates from infrasound data. Journal of Geophysical Research: Atmospheres 118(19):10,707–10,724

Assink J, Pichon AL, Blanc E, Kallel M, Khemiri L (2014a) Evaluation of wind and temperature profiles from ecmwf analysis on two hemispheres using volcanic infrasound. Journal of Geophysical Research: Atmospheres 119(14):8659–8683

Assink J, Waxler R, Smets P, Evers L (2014b) Bidirectional infrasonic ducts associated with sudden stratospheric warming events. Journal of Geophysical Research: Atmospheres 119(3):1140–1153

Assink JD, Waxler R, Drob DP (2012) On the sensitivity of infrasonic traveltimes in the equatorial region to the atmospheric tides. Journal of Geophysical Research 117, DOI 10.1029/2011JD016107

Assink JD, Waxler R, Velea D (2017) A wide-angle high mach number modal expansion for infrasound propagation. Journal of the Acoustical Society of America

Bertin M, Millet C, Bouche D (2014) A low-order reduced model for the long range propagation of infrasounds in the atmosphere. The Journal of the Acoustical Society of America 136(1):37–52, DOI http://dx.doi.org/10.1121/1.4883388

Blom PS, Marcillo OE (2017) An optimal parametrization framework for infrasonic tomography of the stratospheric winds using non-local sources. Geophysical Journal International 208(3):1557, DOI 10.1093/gji/ggw449

Brekhovskikh LM, Godin O (1999) Acoustics of layered media II: point sources and bounded beams. Springer-Verlag Heidelberg, Germany, 524 pp.

Cansi Y (1995) An automatic seismic event processing for detection and location: The P.M.C.C. method. Geophysical Research Letters 22, DOI 10.1029/95GL00468

Charlton AJ, Polvani LM (2007) A new look at stratospheric sudden warmings. Part I: Climatology and modeling benchmarks. Journal of Climate 20:449–469

Charlton-Perez AJ, Baldwin MP, Birner T, Black RX, Butler AH, Calvo N, Davis NA, Gerber EP, Gillett N, Hardiman S, Kim J, Krüger K, Lee YY, Manzini E, McDaniel BA, Polvani L, Reichler T, Shaw TA, Sigmond M, Son SW, Toohey M, Wilcox L, Yoden S, Christiansen B, Lott F, Shindell D, Yukimoto S, Watanabe S (2013) On the lack of stratospheric dynamical variability in low-top versions of the cmip5 models. Journal of Geophysical Research 118:2494–2505, DOI 10.1002/jgrd.50125

Chunchuzov I, Kulichkov S, Perepelkin V, Popov O, Firstov P, Assink J, Marchetti E (2015) Study of the wind velocity-layered structure in the stratosphere, mesosphere, and lower thermosphere by using infrasound probing of the atmosphere. Journal of Geophysical Research: Atmospheres 120(17):8828–8840

Donn WL, Rind DH (1972) Microbaroms and the temperature and wind of the upper atmosphere. Journal of the Atmospheric Sciences 29:156–172

Drob DP, Picone JM, Garcés MA (2003) The global morphology of infrasound propagation. Journal of Geophysical Research 108(4680)

Drob DP, Emmert JT, Crowley G, Picone JM, Shepherd GG, Skinner W, Hays P, Niciejewski RJ, Larsen M, She CY, Meriwether JW, Hernandez G, Jarvis MJ, Sipler DP, Tepley CA, O'Brien MS, Bowman JR, Wu Q, Murayama Y, Kawamura S, Reid IM, Vincent RA (2008) An empirical model of the earth's horizontal wind fields: HWM07. Journal of Geophysical Research 113(A12304), DOI doi:10.1029/2008JA013668

Drob DP, Meier RR, Picone JM, Garcés M (2010) Inversion of infrasound signals for passive atmospheric remote sensing. In: Le Pichon A, Blanc E, Hauchecorne A (eds) Infrasound Monitoring for Atmospheric Studies, Springer, New York, chap 24, pp 701–732

Drob DP, Broutman D, Hedlin MA, Winslow NW, Gibson RG (2013) A method for specifying atmospheric gravity-wave fields for long-range infrasound propagation calculations. Journal of Geophysical Research 118, DOI 10.1029/2012JD018077

Duvall T, Jeffferies S, Harvey J, Pomerantz M (1993) Time–distance helioseismology. Nature 362(6419):430–432

Evers LG, Siegmund P (2009) Infrasonic signature of the 2009 major sudden stratospheric warming. Geophysical Research Letters 36, DOI 10.1029/2009GL041323, l23808

Evers LG, Wapenaar K, Heaney KD, Snellen M (2017) Deep ocean sound speed characteristics passively derived from the ambient acoustic noise field. Geophysical Journal International DOI 10.1093/gji/ggx061

Fricke JT, Evers LG, Smets PSM, Wapenaar K, Simons DG (2014) Infrasonic interferometry applied to microbaroms observed at the large aperture infrasound array in the netherlands. Journal of Geophysical Research 119, DOI 10.1002/2014JD021663

Fujiwhara S (1916) On the abnormal propagation of sound waves in the atmosphere. Monthly Weather Review 44(8):436–439, DOI 10.1175/1520-0493(1916)44¡436:OTAPOS¿2.0.CO;2

Garcés M, Fee D, McCormack D, Servranckx R, Bass H, Hetzer C, Hedlin M, Matoza R, Yepes H (2007) Prototype ASHE Volcano Monitoring System captures the acoustic fingerprint of stratospheric ash injection. Inframatics 3

Garcés MA, Willis M, Hetzer C, Le Pichon A, Drob DP (2004) On using ocean swells for continuous infrasonic measurements of winds and temperature in the lower, middle, and upper atmosphere. Geophysical Research Letters 31, l19304, doi:10.1029/2004GL020696.

Gibbons SJ, , et al (2015) The european arctic: A laboratory for seismoacoustic studies. Seismological Research Letters 86(3)

Godin OA (2002) An effective quiescent medium for sound propagating through an inhomogeneous, moving fluid. Journal of the Acoustical Society of America 112(4):1269–1275

Godin OA (2006) Recovering the acoustic greens function from ambient noise cross correlation in an inhomogeneous moving medium. Physical Review Letters 97(5):054,301

Godin OA (2014) Dissipation of acoustic-gravity waves: An asymptotic approach. Journal of the Acoustical Society of America 136(EL411):411–417, DOI 10.1121/1.4902426

Godin OA, Zabotin NA, Goncharov VV (2010) Ocean tomography with acoustic daylight. Geophysical Research Letters 37(13), l13605

Haney MM (2009) Infrasonic ambient noise interferometry from correlations of microbaroms. Geophysical Research Letters 36(19), DOI 10.1029/2009GL040179, URL http://dx.doi.org/10.1029/2009GL040179, l19808

Kulichkov S (2002) Nonlinear acoustic phenomena in atmosphere. Nonlinear Acoustics at the Beginning of the 21st Century, 16th International Symposium on Nonlinear Acoustics (ISNA Moscow)

Kulichkov S (2010) On the prospects for acoustic sounding of the fine structure of the middle atmosphere. In: Le Pichon A, Blanc E, Hauchecorne A (eds) Infrasound Monitoring for Atmospheric Studies, Springer, New York, USA, chap 16, pp 511–540

Lalande JM, Sèbe O, Landès M, Blanc-Benon P, Matoza R, Pichon AL, Blanc E (2012) Infrasound data inversion for atmospheric sounding. Geophysical Journal International 190, DOI 10.1111/j.1365-246X.2012.05518.x

Landès M, Ceranna L, Le Pichon A, Matoza RS (2012) Localization of microbarom sources using the ims infrasound network. Journal of Geophysical Research: Atmospheres 117(D6):n/a–n/a, DOI 10.1029/2011JD016684, URL http://dx.doi.org/10.1029/2011JD016684, d06102

Le Pichon A, Blanc E, Drob D, Lambotte S, Dessa JX, Lardy M, Bani P, Vergniolle S (2005) Infrasound monitoring of volcanoes to probe high-altitude winds. Journal of Geophysical Research: Atmospheres 110, d13106

Le Pichon A, Blanc E, Drob DP (2005) Probing high-altitude winds using infrasound. Journal of Geophysical Research 110

Le Pichon A, Assink JD, Heinrich P, Blanc E, Charlton-Perez A, Lee CF, Keckhut P, Hauchecorne A, Rüfenacht R, Kämpfer N, Drob DP, Smets PSM, Evers LG, Ceranna L, Pilger C, Ross O, Claud C (2015) Comparison of co-located independent ground-based middle atmospheric wind and temperature measurements with numerical weather prediction models. Journal of Geophysical Research: Atmospheres 120:8318–8331

Lingevitch J, Collins M, Siegmann W (1999) Parabolic equations for gravity and acousto-gravity waves. Journal of the Acoustical Society of America 105(6):3049–3056

Lobkis OI, Weaver RL (2001) On the emergence of the greens function in the correlations of a diffuse field. The Journal of the Acoustical Society of America 110(6):3011–3017, DOI 10.1121/1.1417528

Lonzaga JB, Waxler R, Assink JD, Talmadge C (2015) Modelling waveforms of infrasound arrivals from impulsive sources using weakly non-linear ray theory. Geophysical Journal International 200:1347–1361, DOI 10.1093/gji/ggu479

Manson AH, Meek C, Koshyk J, Franke S, Fritts D, Riggin D, Hall C, Hocking W, MacDougall J, Igarashi K, Vincent R (2002) Gravity wave activity and dynamical effects in the middle atmosphere (60-90 km): observations from an MF/MLT radar network, and results from the Canadian Middle Atmosphere Model (CMAM). Journal of Atmospheric and Solar-Terrestrial Physics 64(2):65–90

Marcillo O, Johnson JB (2010) Tracking near-surface atmospheric conditions using an infrasound network. The Journal of the Acoustical Society of America 128(1):EL14–EL19, DOI 10.1121/1.3442725

Marcillo O, Arrowsmith S, Whitaker R, Morton E, Scott Phillips W (2014) Extracting changes in air temperature using acoustic coda phase delays. The Journal of the Acoustical Society of America 136(4):EL309–EL314

Marcillo O, Arrowsmith S, Blom P, Jones K (2015) On infrasound generated by wind farms and its propagation in low-altitude tropospheric waveguides. Journal of Geophysical Research: Atmospheres 120(19):9855–9868

Melton BS, Bailey LF (1957) Multiple signal correlators. Geophysics 22(3):565–588

Picone JM, Hedin A, Drob D, Aikin A (2002) NRL MSISE-00 empirical model of the atmosphere: statistical comparisons and scientific issues. Journal of Geophysical Research 107, DOI 10.1029/2002JA009430

Pilger C, Ceranna L (2017) The influence of periodic wind turbine noise on infrasound array measurements. Journal of Sound and Vibration 388:188–200

Randel W, Udelhofen P, Fleming E, Geller M, Gelman M, Hamilton K, Karoly D, Ortland D, Pawson S, Swinbank R, Wu F, Baldwin M, Chanin ML, Keckhut P, Labitzke K, Remsberg E, Simmons A, Wu D (2004) The SPARC intercomparison of middle-atmosphere climatologies. Journal of Climate 17(5):986–1003

Rind DH, Donn WL, Dede E (1973) Upper air wind speeds calculated from observations of natural infrasound. Journal of the Atmospheric Sciences 30:1726–1729

Roux P, Kuperman W (2004) Extracting coherent wave fronts from acoustic ambient noise in the ocean. The Journal of the Acoustical Society of America 116(4):1995–2003

Sambridge M, Mosegaard K (2002) Monte carlo methods in geophysical inverse problems. Reviews of Geophysics 40(3), DOI 10.1029/2000RG000089

Seats KJ, Lawrence JF, Prieto GA (2012) Improved ambient noise correlation functions using welchs method. Geophysical Journal International 188(2):513, DOI 10.1111/j.1365-246X.2011.05263.x

Shapiro NM, Campillo M (2004) Emergence of broadband rayleigh waves from correlations of the ambient seismic noise. Geophysical Research Letters 31(7)

Shaw TA, Shepherd TG (2008) Raising the roof. Nature Geoscience 1:12–13, DOI 10.1038/ngeo.2007.53

Smart E, Flinn EA (1971) Fast frequency-wavenumber analysis and Fisher signal detection in real-time infrasonic array data processing. Geophysical Journal of the Royal Astronomical Society 26:279–284

Smets PSM, Evers LG (2014) The life cycle of a sudden stratospheric warming from infrasonic ambient noise observations. Journal of Geophysical Research: Atmospheres 119(21):12,084–12,099

Smets PSM, Evers LG, Charlon-Perez AJ, Lee CF, Harrison RG (2014) Roadmap on the use of arise data for weather and climate monitoring in europe. Tech. Rep. D5.5, Atmospheric dynamics Research InfraStructure in Europe - ARISE - project, FP7 Grant Agreement nr 284387

Smets PSM, Evers LG, Näsholm SP, Gibbons SJ (2015) Probabilistic infrasound propagation using realistic atmospheric perturbations. Geophysical Research Letters 42:6510–6517, DOI 10.1002/2015GL064992

Smets PSM, Assink JD, Le Pichon A, Evers LG (2016) ECMWF SSW forecast evaluation using infrasound. Journal of Geophysical Research: Atmospheres 121(9):4637–4650

Snieder R (2004) Extracting the greens function from the correlation of coda waves: A derivation based on stationary phase. Physical Review E 69(4):046,610

Snieder R (2006) The theory of coda wave interferometry. Pure and Applied geophysics 163(2):455–473

Snieder R, Trampert J (1999) Inverse problems in geophysics. In: Wirgin A (ed) Wavefield Inversion, Springer Verlag, New York, pp 119–190

Sutherland LC, Bass HE (2004) Atmospheric absorption in the atmosphere up to 160 km. Journal of the Acoustical Society of America 115(3):1012–1030

Szuberla C, Olson J (2004) Uncertainties associated with parameter estimation in atmospheric infrasound arrays. Journal of the Acoustical Society of America 115(1)

Tarantola A (2005) Inverse Problem Theory and Methods for Model Parameter Estimation. Society for Industrial and Applied Mathematics

Trampert J, Leveque JJ (1990) Simultaneous iterative reconstruction technique: Physical interpretation based on the generalized least squares solution. Journal of Geophysical Research: Solid Earth 95(B8):12,553–12,559, DOI 10.1029/JB095iB08p12553, URL http://dx.doi.org/10.1029/JB095iB08p12553

Wapenaar K, Fokkema J (2006) Greens function representations for seismic interferometry. Geophysics 71(4):SI33–SI46

Waxler R, Gilbert K (2006) The radiation of atmospheric microbaroms by ocean waves. Journal of the Acoustical Society of America 119(5):2651–2661

Waxler R, Assink JD, Velea D (2017) Modal expansions for infrasound propagation and their consequences for ground-to-ground propagation. Journal of the Acoustical Society of America

Weaver RL, Lobkis OI (2001) Ultrasonics without a source: Thermal fluctuation correlations at mhz frequencies. Physical Review Letters 87(13):134,301

Weemstra C, Boschi L, Goertz A, Artman B (2012) Seismic attenuation from recordings of ambient noise. Geophysics

Weemstra C, Snieder R, Boschi L (2015) On the estimation of attenuation from the ambient seismic field: inferences from distributions of isotropic point scatterers. Geophysical Journal International 203(2):1054

Whipple F (1926) Audibility of explosions and the constitution of the upper atmosphere. Nature 118:309–313

Zwolak JW, Boggs P, Watson LT (2005) ODRPACK95; a weighted orthogonal distance regression code with bound constraints. Tech. Rep. TR-04-31, Computer Science, Virginia Tech., U.S.A.